



**Original Research Article**

## **Granular Activated Carbon (GAC) Adsorption of Herbicide (Metsulfuron methyl) in Water and Doping Zn-TiO<sub>2</sub> Activated Carbon Coupling with Batch Photocatalytic Oxidation**

**Singto Sakulkhaemaruethai<sup>1</sup>, Nathaporn Areerachakul<sup>\*2</sup>, Jaya Kandasamy<sup>3</sup>,  
Aran Kwanpan<sup>2</sup>, Saravanamuthu Vigneswaran<sup>3</sup>, Tien – Vinh Nguyen<sup>3</sup>, Thi Thu Trang  
Nguyen<sup>4</sup>, Do Van Manh<sup>4</sup>**

<sup>1</sup>Rajamangala University of Technology Thanyaburi, 39 Moo 1, Rangsit-Nakhon Nayok, Klong 6, Thanyaburi, Pathum Thani, Thailand 12110

e-mail: [singto@rmutt.ac.th](mailto:singto@rmutt.ac.th)

<sup>2</sup>Suan Sunandha Rajabhat University, 1 Uthong Nok, Dusit, Bangkok, Thailand

e-mail: [nathaporn.ar@ssru.ac.th](mailto:nathaporn.ar@ssru.ac.th)

<sup>3</sup>Faculty of Engineering, University of Technology Sydney (UTS), P.O. Box 123, Broadway, NSW 2007, Australia

<sup>4</sup>The Vietnam Academy of Science and Technology (VAST) 18 Hoang Quoc Viet, Cau Giay, Ha Noi, Vietnam

### **ABSTRACT**

The granular activated carbon (GAC) filter was found to be very effective as a treatment for the removal of herbicides. The Sips isotherms showed the best fit with 6.6 % error. Fixed-bed column experiments packed with GAC were conducted with different GAC bed heights (5, 10, and 15 cm) and different effluent velocities. The GAC fixed bed column shows the model simulation fits reasonably well during the initial period, and also with a shallow bed depth (5 cm) with a flow rate of 4 m/h. Another set of experiments is GAC and GAC doping Zn with various concentrations to remove herbicides from water. The doped Zn-TiO<sub>2</sub> GAC batch experiments can remove MM in terms of DOC from 60 to 77 % by using different w/v of doped Zn onto TiO<sub>2</sub>-GAC. The highest removal of MM 77 % by using a batch experiment was 0.125 % w/v Zn -TiO<sub>2</sub>.

### **KEYWORDS**

*Herbicide, Granular activated carbon, Adsorption, Sips, Fixed bed, Doped Zn-TiO<sub>2</sub> GAC.*

Cite as: Sakulkhaemaruethai, S., Areerachakul, N., Kandasamy, J., Kwanpan, A., Vigneswaran, S., Vinh, N., Trang, N. T., Van Manh, D., Granular Activated Carbon (GAC) Adsorption of Herbicide (Metsulfuron methyl) in Water and Doping Zn-TiO<sub>2</sub> Activated Carbon Coupling with Batch Photocatalytic Oxidation, Journal of Sustainable Development of Natural Resources Management, 1010625, <https://doi.org/10.13044/j.sdnarema.d1.0625>.

### **INTRODUCTION**

The use of activated carbon, such as a granular activated carbon filter, to remove synthetic organic compounds (SOCs) and organic pollutants from water, is known as a highly efficient but simple technique. GAC adsorption is used when the removal of organic compounds is necessary on a continuous basis and when long contact times are needed for effective removal [1]. The effects of these modifications on the adsorption properties of activated carbons against herbicides, in this case, metsulfuron methyl (MM) in aqueous solution, were analyzed. The idea was to explain the mechanism of the adsorption process. Several studies used aqueous solutions of individual herbicides for one pH value and one (room) temperature [2-5]. The

most common Langmuir and the Freundlich isotherms equations were used for the mathematical description of adsorption equilibria. Some of the works also used Sips. The kinetics of the adsorption process, pseudo-first-order (PFO) and pseudo-second-order (PSO) models, were most often used. For the various pH levels, the adsorption equilibrium capacities of the phenoxy herbicides increased with a decrease in pH of the solution. The adsorption characteristics of phenoxy herbicides from an aqueous solution on the active carbon materials (GAC, F-400) were studied, and the Sips equation was used for adsorption equilibrium isotherms [6]. Another study, which discussed in detail using the Sips equation, was described. Single components of herbicides (2,4-D (2,4-dichlorophenoxy acetic acid) and 2,4-DNP (2,4-dinitrophenylhydrazine) have been measured for adsorption equilibria. The herbicides were dissolved in water and three kinds of GACs (F400, SLS103, and WWL). To simulate isothermal adsorption behavior in a fixed-bed adsorber, the linear driving force approximation (LDFA) model was used and successfully simulated experimental adsorption under various operation conditions [7]. In this study, a single component of herbicides (Metsulfuron methyl) was used in batch and fixed-bed adsorption. The GAC was used for adsorption equilibria and for fixed-bed GAC.

## EXPERIMENTAL SET UP AND DESCRIPTION

Four groups of experiments were conducted. The first set was conducted with granular activated carbon (GAC). The purpose of these experiments was to investigate the single-component equilibrium adsorption of GAC. Adsorption equilibrium experiments were conducted by adding different amounts of GAC, ranging from 0.15 to 2.75 g/L, into a 250 mL flask containing 100 mL of metsulfuron methyl at a concentration of 10 mg/L. All flasks were shaken continuously at room temperature (25 °C) for 72 h on a shaking table at a speed of 130 rpm. After 72 h of shaking, samples were taken from all flasks and filtered through a 0.45 µm filter prior to TOC analysis. The adsorption of GAC was determined using the following equation

$$q = \frac{(C_0 - C_e)V}{M} \quad (1)$$

where  $C_0$  is the initial TOC concentration of metsulfuron methyl (mg/L),  $C_e$  is the final concentration of metsulfuron methyl (mg/L),  $V$  is the volume of the solution (mL), and  $M$  is the weight of GAC (g).

The second set of experiments used GAC in a fixed-bed column. These experiments were conducted using transparent acrylic filter columns with dimensions of 2 cm in diameter and 150 cm in length. The column had outlet pipes along its length and at the bottom of the column. The GAC was packed into the column up to the required depth. The columns were operated in a downflow mode. Feed water was pumped from a water tank to the top of the columns and passed through the filter bed. An overflow outlet was placed above the filter bed to maintain a constant head above the GAC filter bed. Effluent samples were collected from the bottom of the column for analysis. One series of experiments was conducted with different flow rates of 1 M/h, 2 M/h, and 3 M/h with a fixed 5 cm GAC bed depth. Another series of experiments used different bed depths of 5 cm, 10 cm, and 15 cm with a fixed flow rate of 4 M/h. The experimental setup is shown in Figure 1.

Another set of experiments is doping Zn - GAC and using a batch experiment to test the efficiency of adsorption. This experiment uses AR chemical grades which are ethyltrimethylammonium bromide (MW 168.08 g/mol), SRL Co., Ltd., titanium (IV) isopropoxide (MW 284.22 g/mol), Sigma Aldrich, Co., Ltd., acetylacetone (MW 100.12 g/mol), Sigma Aldrich, Co., Ltd., ethanol 99.9 % RLC Labscan, Co., Ltd., and zinc Powder (MW 65.38 g/mol), Kemaus, Co., Ltd.

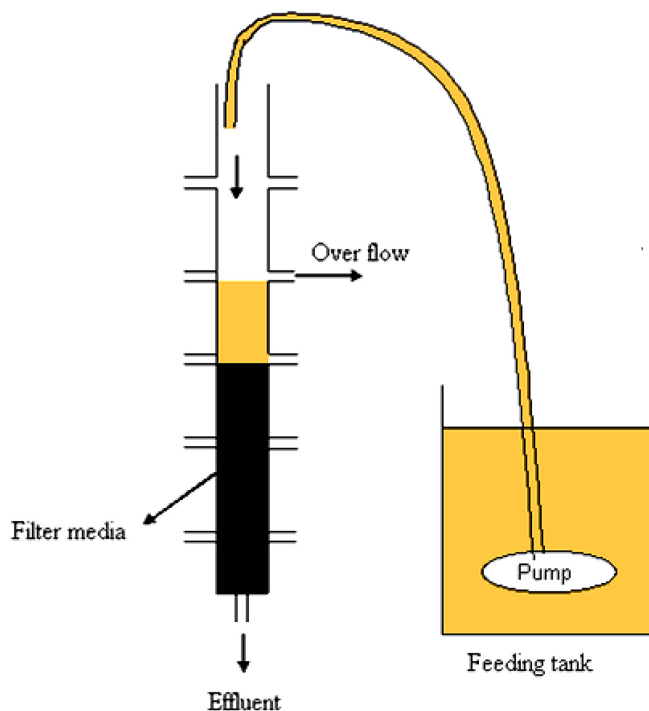
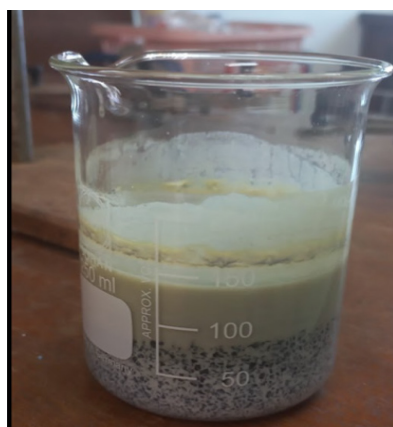
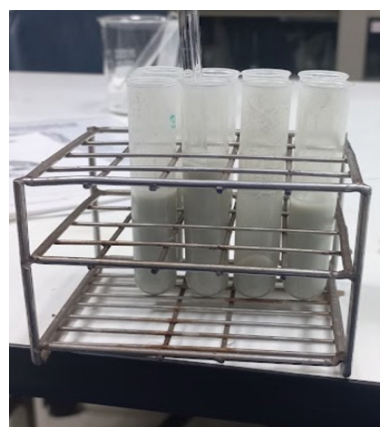


Figure 1. Schematic of GAC column

The furnace used in this experiment is a GALLENKAMP Muffle furnace size 3. The experimental procedure started from coating the activated carbon surface with zinc oxide/titanium dioxide ( $\text{ZnO}/\text{TiO}_2$ ) particles to obtain functional activated carbon (FAC) by sol-gel process using zinc sulfate ( $\text{ZnSO}_4$ ) and titanium (IV) isopropoxide as precursors. Firstly, zinc sulfate ( $\text{ZnSO}_4$ ) solution was prepared by weighing 0.01 g of  $\text{ZnSO}_4$  powder and dissolving it in 80 mL of deionized water.  $\text{ZnSO}_4$  solution concentrations were prepared by weighing  $\text{ZnSO}_4$  powder 0.025 g, 0.1 g, and 0.125 g, respectively. Secondly, a mixture of titanium(IV) isopropoxide and acetylacetone was prepared at a molar ratio of 1:1 and weigh 10 g of acetylacetone and add titanium(IV) isopropoxide to obtain a molar ratio of 1:1. Mix the substances prepared from steps 1 and 2, add 20 mL of ethanol each, and stir the mixture with a magnetic stirrer for 4 h to obtain the activated carbon coating substance. Weighing granular activated carbon and immersing it in an ultrasonic bath for 1 h. Activated carbon is immersed in the coating solution in the ultrasonic bath, and the coating solution and activated carbon are separated by centrifuge, as shown in Figure 2. The activated carbon coating is dried in an oven to remove moisture. The separated clear part is centrifuged, and moisture is removed by oven. Finally, coating activated carbon dried at 500 °C for 1 h.



(A)



(B)

Figure 2. (A-B) 2 A. Sonicated doping  $\text{ZnSO}_4\text{-TiO}_2$  GAC in solution. 2 B. Separated solution

The study of doping GAC with ZnO<sub>4</sub>- TiO<sub>2</sub> (Figure 3) surface after drying at 500 °C by using a scanning electron microscope is shown in Figure 4, using a scanning Electron Microscope, SEM, JEOL, JSM 5410LV, Japan, and operated at 200 kV.

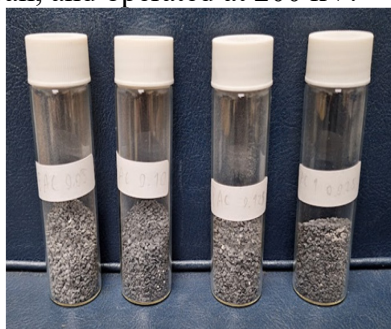


Figure 3. Dried Zn doped- TiO<sub>2</sub> GAC after dried at 500 °C

From the SEM test, it can be observed that the synthetic doped Zn - TiO<sub>2</sub> GAC has different crystal characteristics. This can be observed from the small particles at the nano level on the surface of the GAC, whereas the GAC does not have small particles (Figure 4 A, B, C) at the nano level on the surface of the GAC.

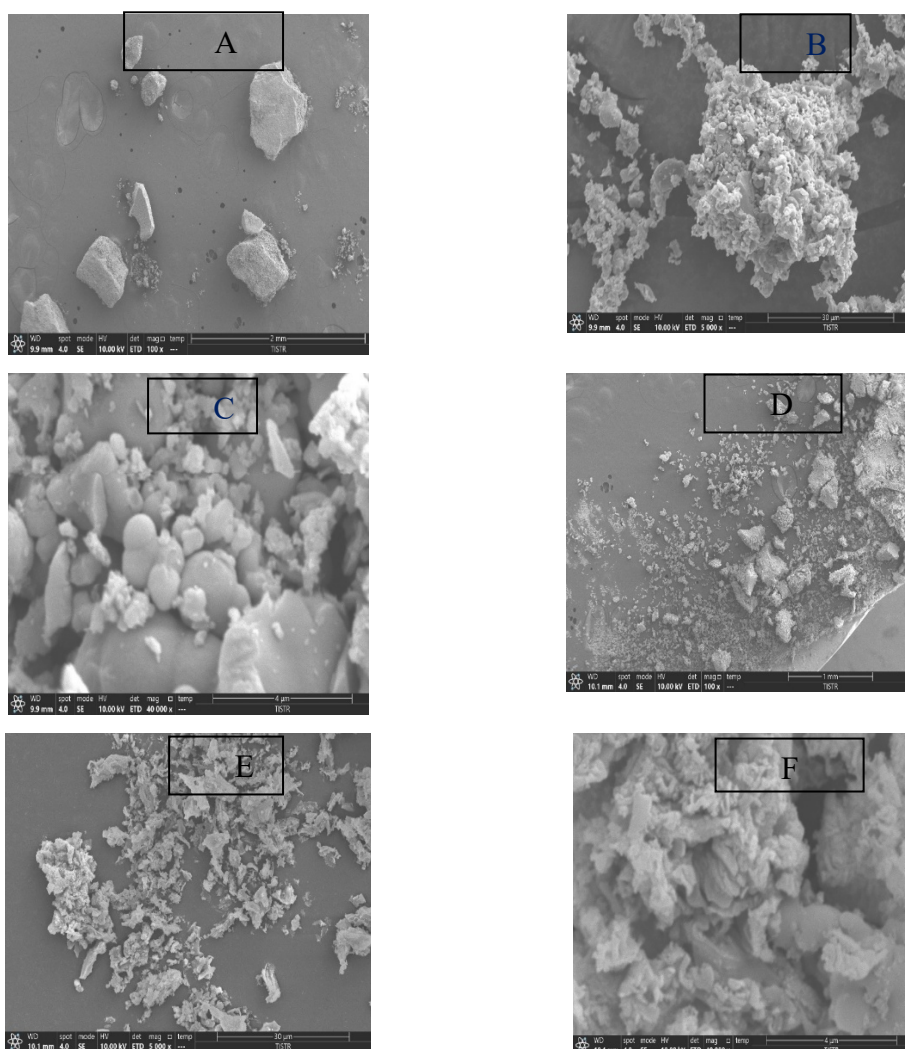


Figure 4. (A – E). Scanning electron microscope of Zn doped TiO<sub>2</sub> - GAC mode SE, detector ETD with different magnify (4A) 100x of doped GAC (4B) 5000x of doped GAC (4C) 40000x of doped GAC (4D) small pellet of doped GAC 100x (4E) small pellet of doped GAC 5000x (4F) small pellet of doped GAC 10000x



Agglomerated Zn on  $\text{TiO}_2$  is not in a different shaped morphology (Figure 4C) at the 40000x of the SEM ETD detector, a simple size of GAC. In the small size of GAC (Figure 4), a similar-shaped morphology of doped Zn- $\text{TiO}_2$  on GAC occurred, as shown in Figure 4F at the 40000x of the SEM ETD detector.

The SEM analysis was used for morphological studies. The SEM images showed the agglomerate-shaped nanomaterials with a varied size range of 30  $\mu\text{m}$ .

The third experiment setup (Figure 5) is batch adsorption for GAC and doped-GAC experiment with a bath/ magnetic stirrer brand PMC model 500 P-2 230 V 0.1 AMP 50 W, to test doped GAC. The 1000 mL beaker contains 10 mg/L metsulfuron methyl (MM) solution at a temperature of 25 °C with tap water in a water bath, and uses a 120 rpm magnetic stirrer to uniformly mix for 1 h. The sample was taken from the pump with the control valve to test DOC.

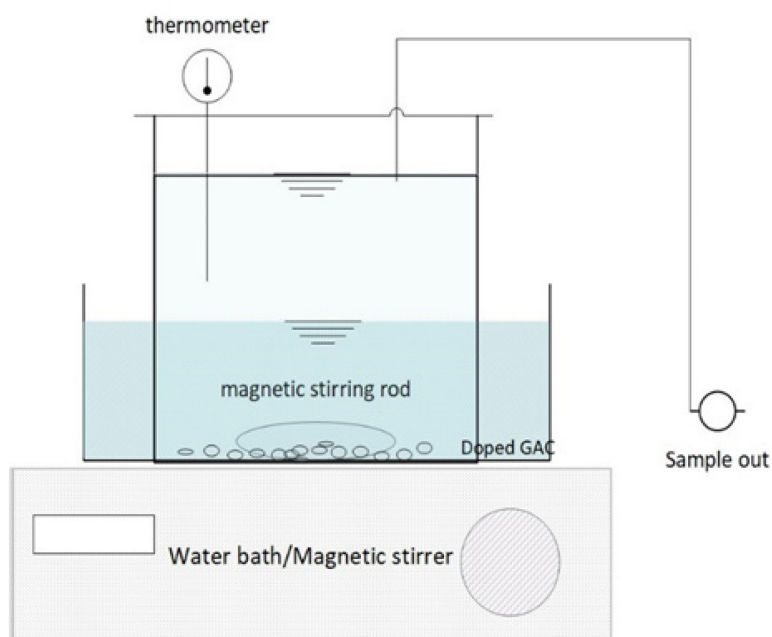


Figure 5. Batch adsorption processes with 25 °C control by tap water in the water batch and 120 rpm

The last experiment is batch photocatalytic oxidation with a UVC submersible UV lamp SOBO T5- UV 5 W, under the same conditions as batch adsorption processes. However, the 1000 mL beaker was covered with foil to protect from the irradiation and irritation of UVC, as shown in Figure 6.

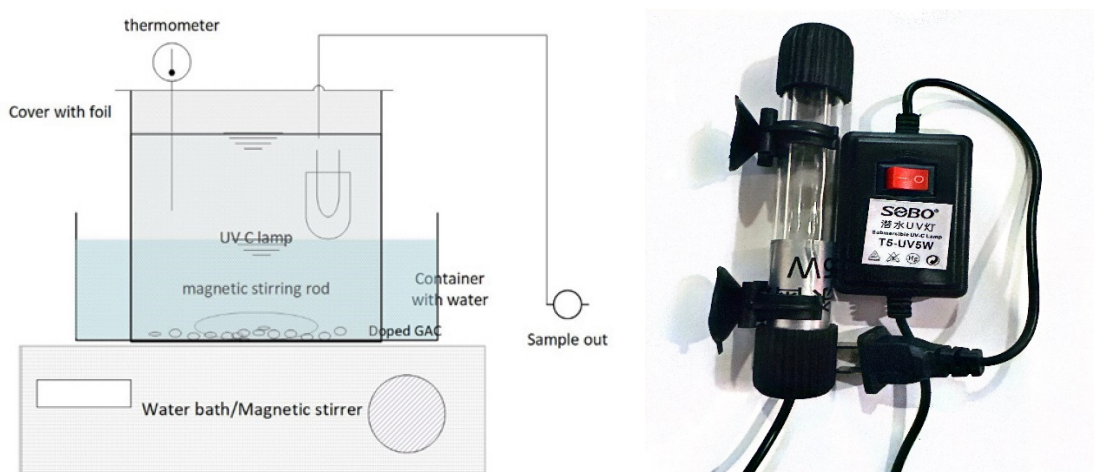


Figure 6. Batch photocatalytic oxidation with 5 W UVC 254 nm, 120 rpm, and 25 °C

## Adsorption equilibrium

A satisfactory description of the equilibrium state between two phases (solid and liquid) is important for a successful representation of the dynamic behaviour of the adsorption system. Various isotherm models were used, including the Langmuir and the Freundlich models, which are the most common isotherm models that describe the equilibrium between the two phases (solid and liquid). These isotherm models are widely accepted because of their simplicity. In addition to these models, an Sip model was also used in the analysis.

### Langmuir isotherm

The development of a Langmuir model is based on the following assumptions [8];

- Adsorption happens in definite localised surface sites;
- Each site binds with only one molecule;
- All identical sorption sites in adsorbent surfaces are energetically uniform and homogeneous: and;
- No interaction occurs among adsorbed molecules.

The Langmuir isotherm is described as

$$q = \frac{aC}{1 + bC} \quad (2)$$

where,

q = amount adsorbed (mg/g)

a, b = isotherm constants

C<sub>e</sub> = equilibrium concentration of metsulfuron methyl (mg/L)

The reciprocal of eq.2 gives,

$$\frac{1}{q} = \frac{1}{ab} + \frac{1}{bC_e} \quad (3)$$

Eq. 3 gives a straight line when 1/C is plotted against 1/q with 1/a as an intercept and 1/b as the gradient.

### Freundlich isotherm

The Freundlich isotherm describes heterogeneous surface adsorption. It differs from the Langmuir isotherm, and the energy distribution for adsorptive sites follows an exponential-type function, which is close to the real situation. Therefore, the rate of adsorption/desorption varies with the strength of the energy at the adsorptive site. The Freundlich isotherm is more accurate than the Langmuir isotherm, but it does not satisfy Henry's law at low surface coverage [9]. The Freundlich isotherm is usually expressed by eq.4 with the following assumptions;

- No association or dissociation of molecules occurs after they are adsorbed on the surface;
- There is a complete absence of chemisorption;

$$q = KC_e^{1/n} \quad (4)$$

where

q = amount adsorption (mg/g)

C<sub>e</sub> = equilibrium concentration of metsulfuron methyl (mg/L)

K<sub>F</sub> = Freundlich isotherm constant (mg/g)

n = Freundlich isotherm constant dimensionless

The logarithm of eq.4 gives

$$\text{Log } q = \text{log } K + (1/n) \text{ log } C_e \quad (5)$$

where  $\log q$  is plotted against  $\log C_e$ ,  $\log K$  is the intercept, and  $1/n$  is the gradient. Figure 7 shows the companion of the Langmuir and the Freundlich isotherms for a system pattern of adsorption of fluoxetine HCl (Prozac) from simulated gastric fluid to Norit USP powdered activated carbon. It can be seen that the Freundlich isotherm has a much sharper rise at low  $C_e$  values (caused by the high-energy sites, which bind well even at low  $C_e$ ).

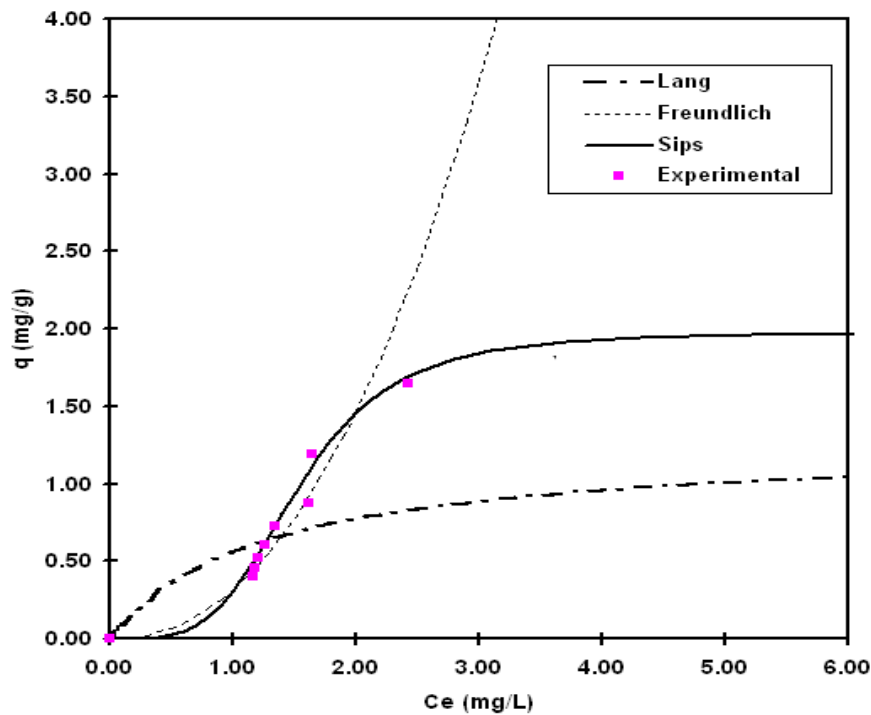


Figure 7. Adsorption equilibrium of metsulfuron methyl by GAC with different isotherm models (contact time = 72 h, mixing rate 130 rpm, temperature 25 °C)

Normally, the Freundlich equation tends to fit data on adsorption from liquid solutions better, while the Langmuir equation sometimes fits data on adsorption of gases to solids a bit better [8]. The Sips isotherm is a model that can be viewed as a combination of both the Langmuir and the Freundlich models. The equilibrium curve obtained from the Sips model is similar to the Freundlich model if the initial solute concentration is low, while at higher solute concentrations, the Sips model follows the Langmuir model. The Sips isotherm model is expressed by eq.6.

$$q = \frac{qmC_e^{\frac{1}{n}}}{1 + K_s C_e^{\frac{1}{n}}} \quad (6)$$

In Eq. 6,  $C$  is the equilibrium organic concentration (mg/L);  $qm$  is the saturation amount of organic adsorbed (mg/g); and  $K_s$  is the Monod half-velocity coefficient.

Adsorption equilibrium experiment of GAC was conducted using a constant concentration of Metsulfuron methyl of 10 mg/L. The purpose of this study was to find the single-component equilibrium concentration of the herbicide. The adsorption behavior was simulated using the Langmuir, the Freundlich, and the Sips isotherms. The adsorption parameters and the coefficients of eqs. 2, 4, and 6 are shown in Table 1.

In this study, the results are shown in Figure 7 indicate that the Sips isotherm describes the GAC equilibrium adsorption reasonably well. The average error between experimental and simulated values was calculated using eq.7.

$$\frac{100}{n} \sum_{i=1}^n \left[ \frac{q_{\text{exp},n} - q_{\text{cal},n}}{q_{\text{exp},n}} \right] \quad (7)$$

where  $q_{\text{exp},n}$  and  $q_{\text{cal},n}$  were respectively, the experimental and calculated values of the amount of adsorption and  $n$  denotes the number of samples.

Table 1. Equilibrium adsorption isotherm parameters

Isotherm models					
Langmuir		Sips		Freundlich	
Parameter	Value	Parameter	Value	Parameter	Value
$q_m$ (mg/g)	1.26	$q_m$ (mg/g)	1.975		
$b$	0.80	$b$	0.185	$k$	0.32
		$n$	0.255	$n$	0.45
%Error	15.72	%Error	6.60	%Error	7.07

The Sips isotherm fitted the experimental data reasonably well with an error of 6.6% compared with 15.72 % and 7.07 % for the Langmuir isotherm and the Freundlich isotherm, respectively. Furthermore, the shape of the curve describing the experimental data shows that with a high concentration of GAC, the isotherm is closer to the Freundlich isotherm. In contrast, at low concentrations of GAC, the trend of the experimental data favours the Langmuir isotherm [10]. Overall, the Sips isotherm gave the best fit with the experimental data because it is essentially a combination of both the Freundlich and the Langmuir models [11].

### Effect of filtration rate in the GAC column

Columns with a 5 cm GAC bed depth were operated at filtration rates of 1, 2, and 4 m/h to study the effect of the filtration rate on TOC removal efficiency (Figure 8.).

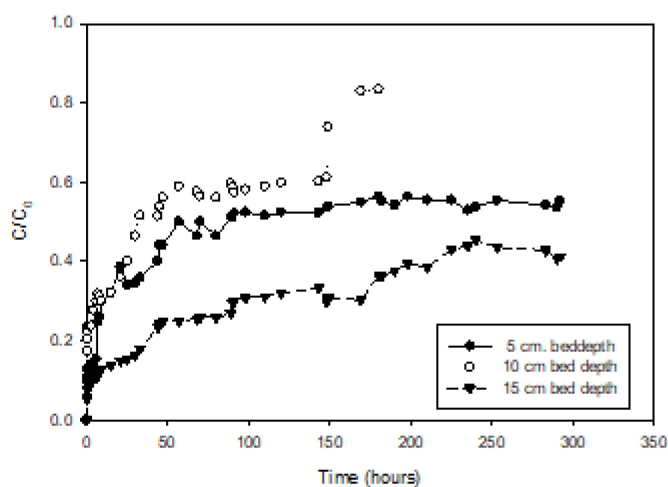


Figure 8. Influence of filtration rate on the performance of adsorption of a 5, 10, 15 cm deep GAC bed. Average influent DOC = 10 mg /L

The efficiency of herbicide removal decreased with the increase in filtration rate. For a GAC filter of 5 cm bed depth and 15 cm bed depth the DOC removal increased from less than 30 % to 60 % when filtration rate decreased from 4 to 1 m/h [12]. The empty bed contact time (EBCT) decreases when the velocity increases in a similar way as Chaudhary *et al.* (2003) in the study with biologically treated sewage effluent (BTSE) [13] claimed that DOC removal increased from 29 to 51.2 % with an increase EBCT from 5 to 20 min [13-15]. For small GAC bed depths of 15 cm, the difference is more clearly apparent when comparing the results at a filtration rate of 4 m/h with 1 m/h but less obvious between filtration rates of 1 m/h and 2 m/h.



## Fixed bed adsorption mathematical model

A mathematical model was developed to simulate the removal efficiency of the GAC fixed-bed adsorption system. The model is principally based on the transport by advection and diffusion processes and adsorption on GAC particles. The adsorbent particles are assumed to be spherical in shape and uniform in size, while the curvature effect of the adsorbent surface was ignored. No biological reaction was assumed to occur. The mass balance equations and the boundary conditions of the fixed bed adsorption system in dynamic conditions are given by the following equations and were previously discussed by Chaudhary *et al.* (2003) [13].

$$\frac{\partial C}{\partial t} = D_{ax} \frac{\partial^2 C}{\partial z^2} - u \frac{\partial C}{\partial z} - \frac{\partial C}{\partial z} - \frac{(1 - \varepsilon_b)}{\varepsilon_b} \frac{3k_f}{R} (C - C_{pi}) \quad (8)$$

where:

The initial and boundary conditions are:-

$C$  = concentration in bulk solution, mg/L

$C_{pi}$  = concentration inside particle, mg/L

$D_{ax}$  = axial dispersion coefficients,  $m^2/s$

$k_f$  = external film mass transfer coefficient of organic, m/s

$R$  = radius of adsorbent particle, m

$u$  = velocity of the fluid, m/s

$z$  = bed depth, m

$\varepsilon_b$  = bed porosity

The initial and boundary conditions are: initial condition,  $C = 0$ , boundary condition:

$$\begin{aligned} \text{at } z=0 \text{ is } D_{ax} \frac{dC}{dz} &= -v(C|_{z=0^-} - C|_{z=0^+}) \\ \frac{dC}{dz} &= 0 \\ \text{and at } z=L \text{ is } \end{aligned} \quad (9)$$

The mass transfer rate was described by the linear driving force approximation (LDFA) model. It was selected because of its simplicity and use of a lumped parameter, such as TOC, to represent the liquid phase concentration of the system. It is assumed in the model that the rate of adsorption to a particle is linearly proportional to a driving force developed from the difference between the concentration at the surface of the particle and the average adsorbed-phase concentration within the particle.

The overall mass balance is given by the following equation.

$$V \frac{dC}{dt} + M \frac{dq}{dt} = 0 \quad (10)$$

The mass transfer equation of the model is given by

$$\frac{dq}{dt} = k_s \cdot (q_s - q) \quad (11)$$

where:

$V$  = volume of the solution in the batch reactor, L

$M$  = weight of the adsorbent, g

$q$  = Average adsorbed phase organic concentration, mg/g

$q_s$  = Adsorbed phase concentration at the external surface of the adsorbent particle, mg/g

$k_s$  = particle phase mass transfer coefficient,  $s^{-1}$

Several isotherms are available in the literature [16]. Figure 7 shows the Sips adsorption isotherm was successful in describing the overall adsorption isotherm of MM. Therefore, in this study, the Sips equation (eq. 12) was used to simulate the adsorption process.

$$q_s = \frac{q_m \cdot b \cdot C^{1/n}}{1 + b \cdot C^{1/n}} \quad (12)$$

where  $q_m$  is the maximum adsorption capacity of the adsorbent, and  $b$  and  $n$  are the constants in the isotherm equation.

The coupled parabolic second-order partial differential equations, eqs. 8 to 11, cannot be solved analytically. Therefore, the preferred means of numerically solving this set of partial difference equations is by the explicit finite difference method using the prescribed boundary conditions.

Table 2 presents the estimated values of the parameters that were used in modelling the GAC filter. The axial dispersion coefficient,  $D_{ax}$  was based on values suggested by Chaudhary *et al.* (2003) [13].  $D_{ax}$  was kept constant while the filter bed depth, TOC influent concentration, and filtration rate were set to match the experimental conditions (see Table 2). The mass transfer coefficients,  $k_f$  and  $k_s$  were obtained by fitting simulated model values to the experimental data.  $k_f$  and  $k_s$  were kept constant for modelling the effect of bed depth (see Figure 9) as it is not believed that these parameters should not vary significantly for this situation [13]. Parameters  $k_f$  and  $k_s$  were varied for modelling the effect of filtration rate, as these parameters are dependent on the fluid velocity and particle diameter [13]. For this case,  $k_f$  was  $1-1.75E^{-5}$  and  $k_s$  was  $1.6E^{-4}$  for both the  $v = 1$  and  $2$  M/h and  $k_s$  was  $4E^{-5}$  for  $v = 4$  M/h (see Figure 9).

Table 2. Parameters used for model simulation of GAC filter;

Parameter	Value				
Bed depth (cm)	5	5	5	10	15
Velocity (M/h)	1	2		4	
TOC of influent (mg/L)	10				
Particle phase mass transfer coefficient, $k_s$ , (x10 <sup>-5</sup> ) (s <sup>-1</sup> )	16			4	
External film mass transfer coefficient $k_f$ (x10 <sup>-5</sup> ) (m/s)	1.5	1.75	1.2*	1.2	
Axial dispersion coefficient $D_{ax}$ (x10 <sup>-5</sup> ) (m <sup>2</sup> /s)	1				
* values of $k_f$ used in Figure 9					

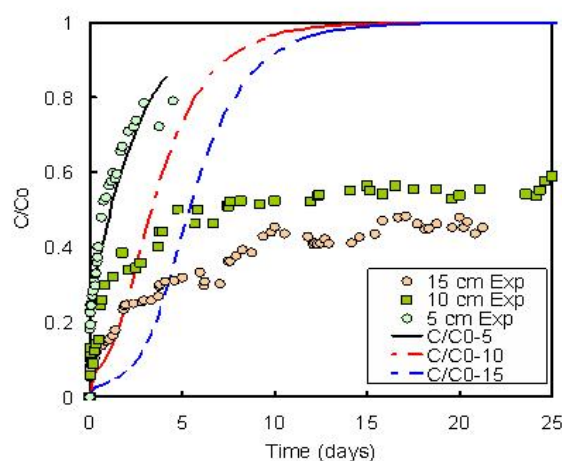


Figure 9. Variation of  $C/C_0$  of the GAC filter for various filter bed depths. Also shown is the fit between experimental data and model simulation for variation in bed depth. Filtration rate = 4 m/h, average influent TOC = 10 mg/L.  $k_f = 1.2e^{-5}$  and  $k_s = 4e^{-8}$  for all modelling runs

Figure 9 shows the fit with experimental data with different filter depths, where the influent concentration and filtration rates were held constant. Here, the performance is expressed in terms of  $C/C_0$ , where  $C$  and  $C_0$  are the concentrations of the effluent and influent, respectively. The modelling parameters were kept constant for all modelling runs. The model is able to simulate the experimental results for bed depths of 5 cm. The modelling for the 10 and 15 cm bed was less successful.

Figure 10 shows the fit with experimental data for the 5 cm bed depth, where the filtration rates were varied. The simulated performance of the GAC filter is shown in Figure 10 fitted reasonably well with the experimental data for velocities of 4 m/h. The modelling for the 5 cm bed with a filtration velocity of 2 and 4 M/h was less successful. It should be noted that this experiment uses the same data as that shown in Figure 9.

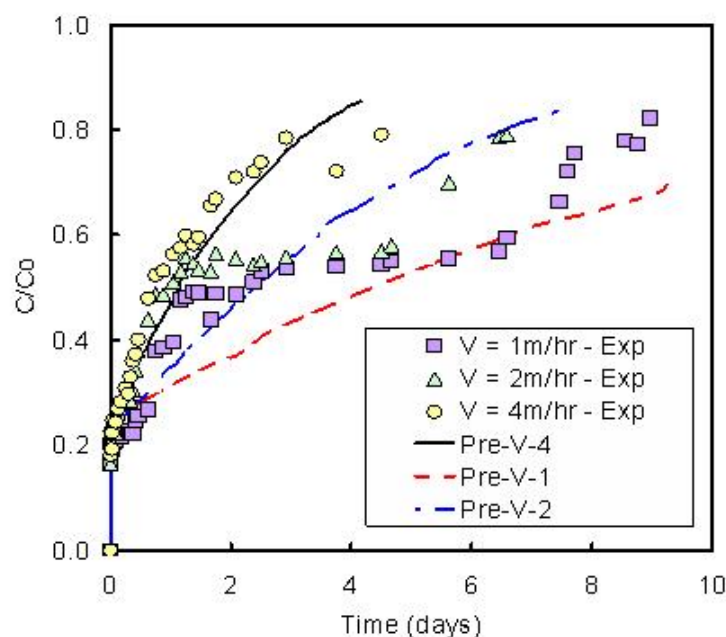


Figure 10. Variation of  $C/C_0$  of the GAC filter for various filtration rates. Also shown is the fit between experimental data and model simulation for variation in bed depth. Bed depth = 5 cm, average influent TOC = 10 mg/L

The model simulation fits reasonably well during the initial period and also with a shallow bed depth (5 cm). This was also observed by Aneeta *et al.* (2000) [17] with a fixed bed depth of less than 10 cm. The isotherm parameters used in this study were lower compared with previous research [17] because of the lower loading of metsulfuron methyl at 10 mg/L. This perhaps implies that the driving force for the GAC desorption of SOC (metsulfuron-methyl) decreases as the isotherm parameter decreases. With a larger GAC bed depth, the exhaustion period, therefore, should be longer compared with smaller bed depths. In this study, a GAC column of 5 cm bed depth was exhausted after 6 days. The DOC of MM removed was 20 % after 4 days, of the comparable values of GAC bed depths of 50 % DOC removal (10 cm) and 67 % DOC removal (15 cm) (Figure 8).

A near steady state occurs after 6 days with a bed depth of 10 and 15 cm. This phenomenon may have resulted from the growth of some microorganism on the GAC surface, especially in the exhausted portion of the GAC [18], and may be attributed to partial biological growth and partial GAC adsorption. This is perhaps because at low concentrations of MM, the aerobic microbial activity is enhanced by the sufficient dissolved organic oxygen in the water ahead of the GAC bed. More generally, all GAC columns act as biofilters because GAC appears to remove any disinfectant in the top few centimeters of the bed. Some studies report that small values of the

Freundlich isotherm slope present the possibility of small concentration gradients and significant irreversible adsorption to the GAC [11-12,19]. The driving force for desorption of GAC is critical because of the very short period of time available to transport the SOC's to the microorganism on the external GAC surface. Microbiology may also vary temporally and spatially within the GAC column. Depending on the point in its service life, a GAC column can contain three zones of varying length: exhausted GAC, partially exhausted GAC, and virgin GAC.

Unfortunately, very little work has been done on the biodegradation and non-biodegradation of herbicide SOC's. Some research has shown that inoculated microorganisms can adsorb triazine and s-triazine in surface water [20]. Many nonbiodegradable SOC's may cause adverse health effects, but this lack of research in the area of microorganism growth on GAC with sulfonyl urea herbicides is important and needs further research.

### Batch adsorption doped Zn – TiO<sub>2</sub> GAC

The adsorption of C/C<sub>0</sub> doped Zn – TiO<sub>2</sub> GAC 0.025 %, 0.1 %, and 0.125 % is fluctuated compared with GAC alone. So, in this experiment (Figure 11), doped Zn-TiO<sub>2</sub> GAC was not simulated with the model. These phenomena may occur from desorption of MM during the first period 20 min of adsorption [21]. The removal of MM in terms of DOC was in the range of 60 – 70 % while the highest removal of MM in terms of DOC was 77 % with the doped Zn-TiO<sub>2</sub> GAC 0.125 % w/v. After that, MM was brought to put a batch photocatalytic hybrid system.

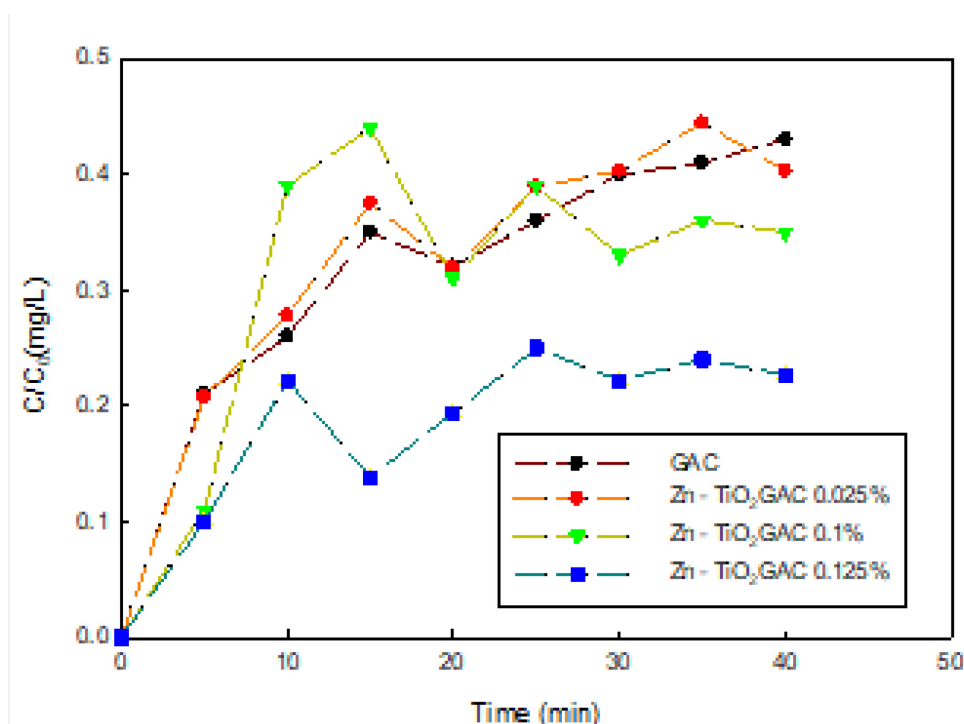


Figure 11. Variaton of C/C<sub>0</sub> GAC and doped Zn-TiO<sub>2</sub> GAC with 0.025 %, 0.1 % and 0.125 % W/V (1 mg/L, 120 rpm, 25 °C)

### Batch photocatalysis hybrid system

A batch photocatalysis hybrid system was set up, as shown in Figure 12. The treated MM solution was put in the batch photocatalysis system. In the batch photocatalysis system, UV C light was turn off for 30 min. The doped Zn–TiO<sub>2</sub> GAC with 0.125 % W/V 1 g/L was put in the batch system at 120 rpm, covered with aluminum foil. The temperature was controlled by tap water in a water bath at about 25 °C. To observe the dark adsorption process. The desorption of

MM solution in terms of dissolved organic carbon occurred during the first period of 30 min without UV [22]. After turning on the UVC, the photo-catalytic oxidation can remove MM to zero within 30 min of operation.

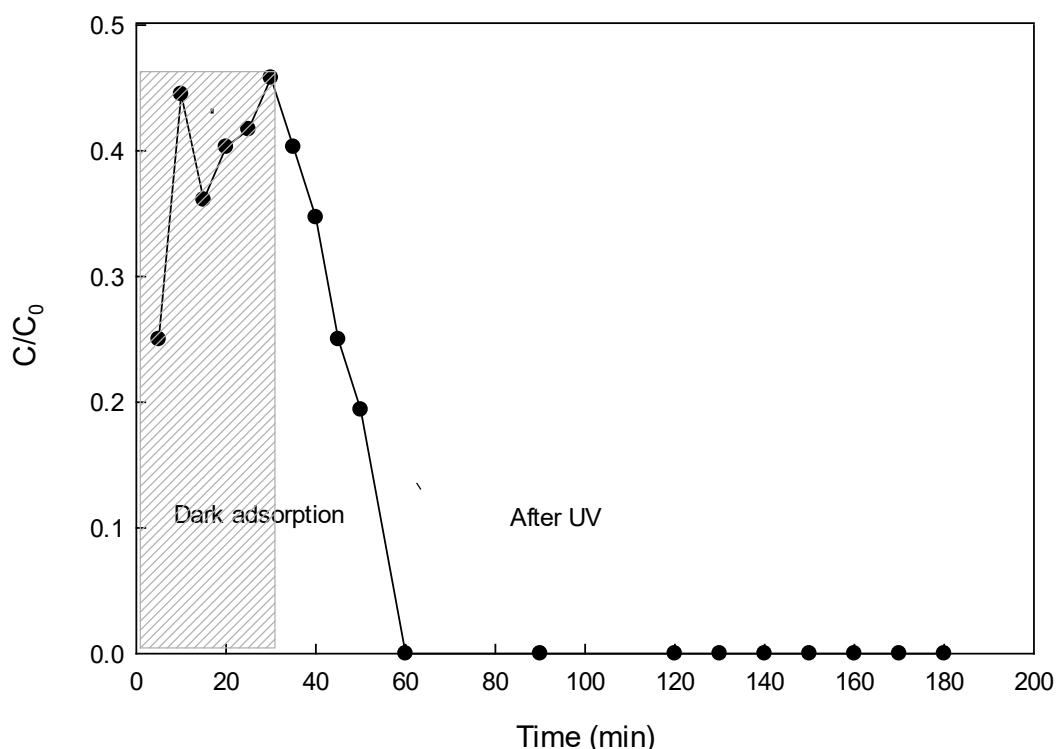


Figure 12.  $C/C_0$  of MM solution after 0.125 %W/V adsorption couple with batch photocatalysis hybrid system UVC 254 nm 5 watts, 120 rpm, 25°C, covered with aluminum foil

## CONCLUSIONS

The 10 and 15-cm deep GAC columns showed a steady state of effluent concentration. Modelling using GAC adsorption theory could not replicate the experimental results. This phenomenon is attributed to the formation of microorganisms (BAC) on the surface of GAC in addition to GAC adsorption. Freundlich and Sips isotherm parameters are relatively small. It means that with 10 and 15 cm GAC bed depths. The GAC in the column was not fully exhausted because the parameters of the isotherm Freundlich and Sips models are small, and the exhaustion time is extensive. The doped Zn – TiO<sub>2</sub> GAC batch experiments can remove MM in term of DOC from 60 to 77 % by using different w/v of doped Zn onto TiO<sub>2</sub> – GAC. The highest removal of MM 77 % by using a batch experiment was 0.125 % w/v Zn -TiO<sub>2</sub> GAC, which was hybridized with the photocatalytic oxidation process by using UV-C, and under the same conditions as the batch experiment, covering with aluminium foil can eradicate the least of the MM solution.

For future work, the fixed bed depth of GAC doping with Zn – TiO<sub>2</sub> should be done with different AOPs systems, such as semi-batch and continuous systems. Finally, Membrane hybrid systems should be provided, coupled with a fixed-bed column and photocatalytic oxidation



## ACKNOWLEDGMENT(S)

The authors would like to thank Thailand Science Research and Innovation for supporting this project.

## NOMENCLATURE

q	amounted adsorption	[mg/g]
a, b	Isotherm constant	
C <sub>e</sub>	equilibrium concentration of metsulfuron methyl	[mg/L]
K <sub>F</sub>	Freundrich isotherm constant	[mg/g]
n	Freundrich isotherm constant dimensionless	
q <sub>m</sub>	saturation amount of organic adsorbed	[mg/g]
K <sub>s</sub>	Monod half velocity coefficient	
q <sub>exp.</sub>	Experimental of the amount of adsorption	[mg/g]
q <sub>cal</sub>	Calculation of the amount of adsorption	[mg/g]
C	concentration in bulk solution	[mg/L]
C <sub>pi</sub>	concentration inside the particle	[mg/L]
D <sub>ax</sub>	axial dispersion coefficients	[m <sup>2</sup> /s]
k <sub>f</sub>	external film mass transfer coefficient of organic	[m/s]
R	radius of the adsorbent particle	[m]
u	velocity of the fluid	[m/s]
z	bed depth	[m]
ε <sub>b</sub>	bed porosity	[m]
V	volume of the solution in batch reactor	[L]
M	weight of the adsorbent	[g]
q	Average adsorbed phase organic concentration	[mg/g]
q <sub>s</sub>	Adsorbed phase concentration at the external surface of adsorbent particle	[mg/g]
k <sub>s</sub>	particle phase mass transfer coefficient	[s <sup>-1</sup> ]

## REFERENCES

1. P. Luekittisup, V. Tanboonchaay, J. Chumee, S. Predapitakkun, R. W. Kiatkomol, and N. Grisdanurak, "Removal of Chlorinated Chemicals in H<sub>2</sub> Feedstock Using Modified Activated Carbon", *Journal of Chemistry*, Vol. 2015, pp. 1–9, 2015, <https://doi.org/10.1155/2015/959012>.
2. M. Yang, J. Hubble, A. D. Lockett, and R. R. Rathbone, "Thermal monitoring of phenoxyacid herbicide adsorption on granular activated carbon", *Water Research*, Vol. 31, No. 9, pp. 2356–2362, 1997, [https://doi.org/10.1016/S0043-1354\(97\)00086-9](https://doi.org/10.1016/S0043-1354(97)00086-9).
3. A. Derylo-Marczewska, M. Blachnio, A. W. Marczewski, M. Seczkowska, and B. Tarasiuk, "Phenoxyacid pesticide adsorption on activated carbon – Equilibrium and kinetics",

- Chemosphere, Vol. 214, pp. 349–360, 2019, <https://doi.org/10.1016/j.chemosphere.2018.09.088>.
4. W. Kaminski, K. Kusmierk, and A. Swiatkowski, “Sorption equilibrium prediction of competitive adsorption of herbicides 2,4-D and MCPA from aqueous solution on activated carbon using ANN”, Adsorption, Vol. 20, No. 7, pp. 899–904, 2014, <https://doi.org/10.1007/s10450-014-9633-9>.
  5. K. Kuśmierk, A. Świątkowski, K. Skrzypczyńska, and L. Dąbek, “Adsorptive and Electrochemical Properties of Carbon Nanotubes, Activated Carbon, and Graphene Oxide with Relatively Similar Specific Surface Area”, Materials, Vol. 14, pp. 496–506, , 2021, <https://doi.org/10.3390/ma14030496>.
  6. T.-Y. Kim, S.-S. Park, S.-J. Kim, and S.-Y. Cho, “Separation characteristics of some phenoxy herbicides from aqueous solution”, Adsorption, Vol. 14, No. 4–5, pp. 611–619, 2008, <https://doi.org/10.1007/s10450-008-9129-6>.
  7. S. Y. Cho, S. J. Kim, T. Y. Kim, H. Moon, and S. J. Kim, “Adsorption characteristics of 2,4-dichlorophenoxyacetic acid and 2,4-dinitrophenol in a fixed bed adsorber”, Korean J. Chem. Eng., Vol. 20, No. 2, pp. 365–374, 2003, <https://doi.org/10.1007/BF02697254>.
  8. D. O. Cooney, Adsorption design for wastewater treatment. Boca Raton, FL, USA: Lewis Publishers, CRC Press, 1999, ISBN 978-1566703338.
  9. G. McKay, Ed., Use of adsorbents for the removal of pollutants from wastewaters. Boca Raton, FL, USA: CRC Press, 1996.
  10. K. Kuśmierk, L. Dąbek, and A. Świątkowski, “Comparative study on the adsorption kinetics and equilibrium of common water contaminants onto bentonite”, Desalination and Water Treatment, Vol. 186, pp. 373–381, 2020, <https://doi.org/10.5004/dwt.2020.25476>.
  11. K. Kuśmierk, A. Białek, and A. Świątkowski, “Effect of activated carbon surface chemistry on adsorption of phenoxy carboxylic acid herbicides from aqueous solutions”, Desalination and Water Treatment, Vol. 186, pp. 450–459, 2020, <https://doi.org/10.5004/dwt.2020.25645>.
  12. N. Ye, N. Cimetiere, V. Heim, N. Fauchon, C. Feliers, and D. Wolbert, “Upscaling fixed bed adsorption behaviors towards emerging micropollutants in treated natural waters with aging activated carbon: Model development and validation”, Water Research, Vol. 148, pp. 30–40, 2019, <https://doi.org/10.1016/j.watres.2018.10.029>.
  13. D. S. Chaudhary, S. Vigneswaran, V. Jegatheesan, H. H. Ngo, H. Moon, W. G. Shim, and S. H. Kim, “Granular activated carbon (GAC) adsorption in tertiary wastewater treatment: experiments and models”, Water Science and Technology, Vol. 47, No. 1, pp. 113–120, 2003, <https://doi.org/10.2166/wst.2003.0030>.
  14. M. W. LeChevallier, W. C. Becker, P. Schorr, and R. G. Lee, “Evaluating the Performance of Biologically Active Rapid Filters”, Journal AWWA, Vol. 84, No. 4, pp. 136–146, 1992, <https://doi.org/10.1002/j.1551-8833.1992.tb07339.x>.
  15. B. K. Pramanik, F. A. Roddick, and L. Fan, “Effect of biological activated carbon pre-treatment to control organic fouling in the microfiltration of biologically treated secondary effluent”, Water Research, Vol. 63, pp. 147–157, 2014, <https://doi.org/10.1016/j.watres.2014.06.014>.
  16. C. Tien, Adsorption calculations and modeling. Boston, USA: Butterworth-Heinemann, 1994.
  17. B. Aneeta, Adsorption and adsorption hybrid system in removal of herbicide, PhD Dissertation, University of Technology, Sydney, Australia, 2000.
  18. A. R. H. Putz, D. E. Losh, and G. E. Speitel, “Removal of Nonbiodegradable Chemicals from Mixtures during Granular Activated Carbon Bioregeneration”, J. Environ. Eng., Vol. 131, No. 2, pp. 196–205, 2005, [https://doi.org/10.1061/\(ASCE\)0733-9372\(2005\)131:2\(196\)](https://doi.org/10.1061/(ASCE)0733-9372(2005)131:2(196)).
  19. A. Y. L. Li, and F. A. DiGiano, “Availability of Sorbed Substrate for Microbial Degradation on Granular Activated Carbon”, Journal (Water Pollution Control Federation), Vol. 55, No. 4, 1983, pp. 392–399.
  20. S. J. Feakin, E. Blackburn, and R. G. Burns, “Biodegradation of s-triazine herbicides at low concentrations in surface waters”, Water Research, Vol. 28, No. 11, pp. 2289–2296, 1994, [https://doi.org/10.1016/0043-1354\(94\)90044-2](https://doi.org/10.1016/0043-1354(94)90044-2).

- 21.N. Areerachakul, S. Vigneswaran, H. H. Ngo, and J. Kandasamy, “Granular activated carbon (GAC) adsorption-photocatalysis hybrid system in the removal of herbicide from water”, *Separation and Purification Technology*, Vol. 55, No. 2, pp. 206–211, 2007, <https://doi.org/10.1016/j.seppur.2006.12.007>.
- 22.L. Erdei, N. Arecrachakul, and S. Vigneswaran, “A combined photocatalytic slurry reactor–immersed membrane module system for advanced wastewater treatment”, *Separation and Purification Technology*, Vol. 62, No. 2, pp. 382–388, 2008, <https://doi.org/10.1016/j.seppur.2008.02.003>.



Paper submitted: 16.07.2025

Paper revised: 05.09.2025

Paper accepted: 05.09.2025